International Journal of Advances in Applied Sciences (IJAAS)
Vol. 9, No. 3, September 2020, pp. 211~219
ISSN: 2252-8814, DOI: 10.11591/ijaas.v9.i3.pp211-219

Spectroscopic properties of lithium borate glass containing Sm^{3+} and Nd^{3+} ions

I. Kashif[1], A. Ratep[2], S. Ahmed[3]
[1]Faculty of Science, Department of Physics, Al-Azhar University, Egypt
[2.3] Faculty of womens for arts, Science& Education, Department of Physics, Ain Shams University, Egypt

Article Info

Article history:

Received Jan 24, 2020
Revised Apr 23, 2020
Accepted May 11, 2020

Keywords:

Borate glass containing $Sm3^{+}$ and Nd^{3+} ion
DTA
FTIR
Optical properties
XRD

ABSTRACT

Lithium borate glass samples mixed with a different concentration of Sm^{3+} and Nd^{3+} ions organized by quenching technique. Structural, vibration groups and spectral properties of glass samples investigated using X-ray diffraction, FTIR, UV/Vis/NIR and photoluminescence spectroscopy. The X-ray confirmed the lithium borate glass samples containing Sm^{3+} and Nd^{3+} ions in the amorphous state. Luminescence spectra of glass samples excited at 400 nm recorded, here three luminescence bands observed in Visible region, which due to spectra materials (Sm3+, Nd3+). These indicate that these glass samples responsible orange emission and used in the improvement of materials for LED, and optical devices. The functional vibration groups of the glass matrix studied using FTIR spectroscopy.

Corresponding Author:

I. Kashif,
Department of Physics,
Al-Azhar University,
Nasr City, Cairo, Egypt.
Email: ismailkashif52@yahoo.com

1. INTRODUCTION

Borate glasses act as host substances for studies the character, structure of the luminescence and useful practical applications. Specifically, the borate glass, free and containing rare earth or transition elements is a promising substance for nonlinear optics, quantum electronics, laser generation, scintillations, thermoluminescent dosimeters, detectors, transformers of the ionizing radiation, and many other applications [1-11].

Borate glasses are vital glass formers and perform a major function in diverse applications. The BO_3 group's vibration and non-bridging oxygen (NBOs) increases in borate glass structure when the B_2O_3 content increase from 10 mol% to 30 mol% [12-14]. Silicate glasses are a host material for the luminescence of rare-earth and transition metal ions, because of the silicate glasses good optical and mechanical properties in addition to excellent chemical durability [15]

The physical and spectroscopic properties of lithium borate glasses containing Sm^{3+} studied. And the rise of Sm^{3+} content in glass samples increases the glass sample density due to the formation of BO_4 modules. The number of transitions peaks defined within the absorption spectra of glass containing Sm^{3+} compared to samarium-free glass. These glass samples emitted sturdy peak at 598 nm which corresponds to $^4G_{5/2} \rightarrow {}^6H_{7/2}$ transition. This indicates that these samples of glass can adjust for LED applications [16, 17]. From rare-earth ions, the Sm^{3+} ion is considerable, Sm^{3+} ion growing stipulate in various fluorescent gadgets, high-density optical storage, color displays, undersea communication and visible solid-state lasers because of its vivid emission in orange-red areas [18]. The $^4G_{5/2}$ level of Sm^{3+} possesses relatively high quantum

efficiency and indicates numerous populating in addition to quenching emission channels [19]. Some authors studied the optical properties of Sm^{3+} ion-doped various host glass networks [20-22]. Neodymium is one of the maxima studied rare-earth ions and discovered to have vast applications in photonic gadgets [23, 24].

From the mentioned above and other many studies of synthetic and optical and physical properties have made on different types of glass groups containing component Nd^{3+} or Sm^{3+}. But there have few studies of their presence together in the glass samples. The effect of changing the ratio of one of them with the stability of the ratio of the second element studied. It found that the emission intensity decreased by increasing the ratio of Nd^{3+} with the constant of Sm^{3+}. As well as the emission intensity increase with increasing of Sm^{3+} and constant of Nd^{3+} content [25, 26].

In this study, we study the effect of replacing Sm^{3+} by Nd^{3+} on the structural, thermal, optical, spectroscopic properties of Sm^{3+} and Nd^{3+} ions on this glass. Judd-ofelt parameters calculated, for observed absorption spectra for Sm^{3+} and Nd^{3+} ions as well as the emission intensity.

2. EXPERIMENTAL WORK

Sm^{+3} and Nd^{3+} doped ion synthesized in the Borate glass system by conventional melt quenching method. The starting chemicals used reagent grade of H_3BO_3, Li_2CO_3, Sm_2O_3, and Nd_2O_3 with 99.99% purity. Chemical compositions prepared glasses as shown in Table 1.

Table 1. The code and glass sample's composition (mol %).

Sample no.	Mol %			
	Li_2O	B_2O_3	Nd_2O_3	Sm_2O_3
1	33	66	1	-
2	33	66	0.75	0.25
3	33	66	0.5	0.5
4	33	66	0.25	0.75
5	33	66	-	1

The mixture melted in porcelain crucibles at the 1100 ^{O}C for 2h. The structure of each sample confirmed amorphous by X-ray diffraction with a Phillips diffractometer PW3700 using CuKα1 radiation. The density measured using the Archimedes method. Optical absorption spectra of samples recorded using the UV-Vis spectrometer (Model-JASCO V570). The IR spectra of the glasses recorded using the FTIR 4100 JASCO spectrophotometer Michelson interferometer type in the wavenumber region from 400 to 2000 cm^{-1}. The Differential thermal analysis of glass samples carried using a SHIMADZUDTA-50 ANALYZER. The emission measure using Spectrofluorometer type JASCO-FP-6300.

3. RESULTS AND DISCUSSION

Figure 1 demonstrates the XRD of the prepared glass sample containing a different Nd and Sm oxide content. That indicates the amorphous nature of the samples.

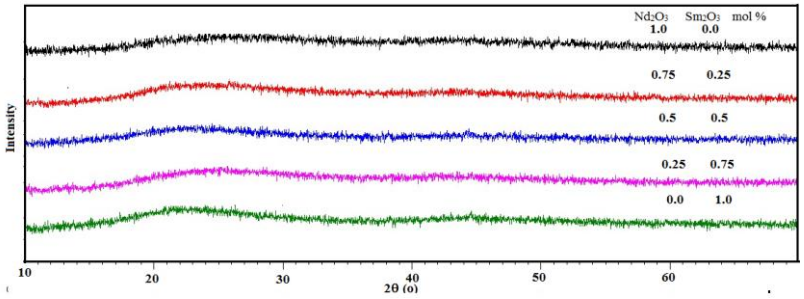

Figure 1. The XRD of glass sample containing a different concentration of Nd and Sm oxides.

The glass density tendency increase with the increase of Sm_2O_3 content as shown in Figure 2. It's due to the structural atom arrangement change when Sm_2O_3 substitute Nd_2O_3 in the Li_2O-B_2O_3 glass network,

and the density of Sm_2O_3 (8.347 g/cm^3) greater than the density of Nd_2O_3 (7.24 g/cm^3). The excess density of the samples is due to the molecular weight of the samarium higher than any other component in the glass samples.

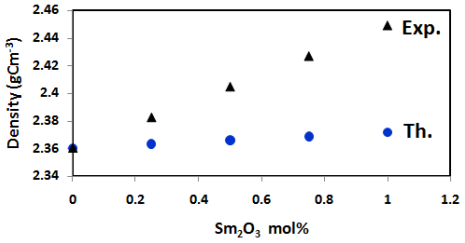

Figure 2. The relation between the density and samarium oxide content

Figure 3 shows the DTA curves obtained for Sm_2O_3- Nd_2O_3 doped lithium borate glass. This figure indicates the presence of endothermic peak Tg (glass transition temperature), the exothermic peak Tc (the crystallization temperature) and the endothermic peak Tm (melting temperature) which tabulated in Table 2. The Tg represents the strength or rigidity of the glassy structure [27].

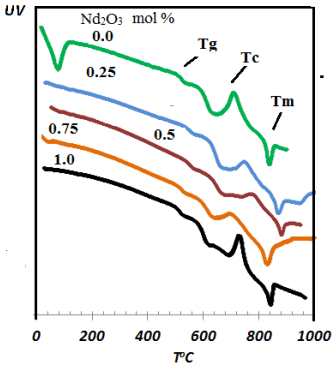

Figure 3. The DTA curve of glass samples.

The difference (△x) among Tx and Tg which employ the glass forming ability [28].

Table 2. Thermal stability, the glass transition, start crystallization, crystallization and melting temperatures

sample	Tg(°C)	Tx(°C)	Tm(°C)	Δx(°C)
1	519	689	839	170
2	533	671	828	138
3	529	697	832	168
4	530	676	822	146
5	530	646	835	116

According to DTA curves, the values of Δx calculated. The impact substitution of Nd with Sm on the glass-forming ability can appear. From Table 2, observed that the quantity of Δx of all samples > 100, it means that all glass samples have glass-forming ability and thermal stability. Figure 4 shows the FTIR spectra of glasses doped with Nd^{3+} and Sm^{3+} ion with different concentrations. Three areas defined the borate glass transmission spectra, the band (1200 - 1600 cm^{-1}) is the primary region, the second region from 800 to 1200 cm^{-1} and the last from 600 to 800 cm^{-1}.

Where the primary bands are the stretching, relaxation of the B—O bond of trigonal BO_3 units, the second attributed to BO_4units, and the third due to the bending vibrations of B—O—B linkages inside the borate network [29-31]. The rare earth oxides doped borate glass outcomes within the conversion of BO_3

units into tetrahedral BO_4 units, and create non-bridging oxygen. Every BO_4 unit connected two different units, the band at 485 cm^{-1} due O−Sm or Nd shifted to higher wavenumber with the growing attention of Sm.

Figure 5 shows the Vis-NIR absorption spectrum acquired from the lithium borate glasses doped Nd^{3+} and Sm^{3+} with different concentrations. Figure 5 shows eight electronic f - f transition bands of Nd^{3+} in Table 3. This result compared with the prior referenced recommendations [32]. Figure 6 shows the optical absorption spectra of the lithium borate glass doped with 1 mol % Sm_2O_3 or Nd_2O_3. The observed absorption bands assigned to appropriate fitting electronic f—f transitions inside Sm^{3+} ion as shown in Table 4.

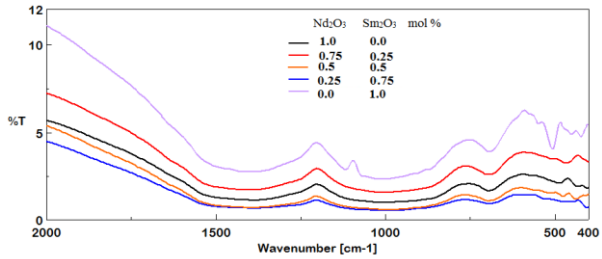

Figure 4. The IR spectra of glasses doped with Nd^{3+} and Sm^{3+} ion with different concentrations

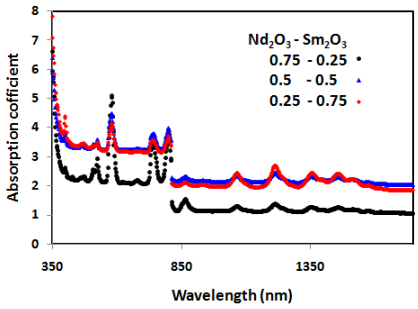

Figure 5. The Vis-NIR absorption spectrum obtained from the lithium borate glasses doped Nd^{3+} and Sm^{3+} with different concentrations

Table 3. The 4f transition levels of Nd^{3+} doped in lithium borate glasses compared with the reported (Rai and Rai 2006).

Transition $^4I_{9/2} \rightarrow$	Wavelength (nm)	Wavenumber (cm^{-1})	Wavenumber reported (cm^{-1})
$^2P_{1/2}$	428	23365	23140
$^2G_{9/2}$	472	21186	21171
$^4G_{9/2}$	510	19607	19544
$^4G_{7/2}$	524	19084	19018
$^4G_{5/2}$	582	17182	17167
$^2H_{11/2}$	624	16026	16026
$^4F_{9/2}$	680	14706	14854
$^4S_{3/2}$	746	13405	13460
$^4F_{5/2}$	802	12469	12573
$^4F_{3/2}$	868	11521	11527

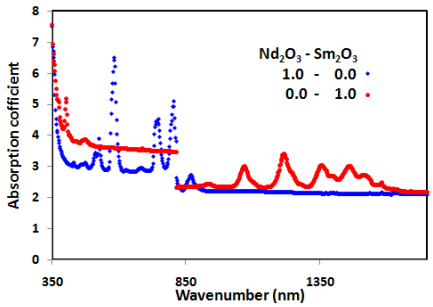

Figure 6. The optical absorption spectra of the lithium borate glass doped with 1 mol % Sm_2O_3 or Nd_2O_3

Table 4. The 4f transition levels of Sm^{3+} doped in lithium borate glasses

Transition	Wavelength(nm)	Wavenumber(cm^{-1})
$^6H_{5/2}\rightarrow {}^4F7/2$	400	25000
$^6H_{5/2}\rightarrow {}^6F9/2$	1066	9380
$^6H_{5/2}\rightarrow {}^6F7/2$	1214	8237
$^6H_{5/2}\rightarrow {}^6F5/2$	1358	7363
$^6H_{5/2}\rightarrow {}^6F3/2$	1458	6858

The optical spectra of glass contain combined Nd_2O_3 and Sm_2O_3 indicates fifteen distinct absorption bands at 346, 428, 472, 510, 524, 582, 680, 746, 802, 868, 400, 1066, 1214, 1358, and 1458 nm which due to the transitions of $^4I_{9/2} \rightarrow {}^4D_{1/2}$, $^2P_{1/2}$, $2G_{9/2}$, $4G_{9/2}$,$4I_{9/2}\rightarrow 4G_{7/2}$, $4I_{9/2} \rightarrow 4G_{5/2}$, $4F_{9/2}$, $4S_{3/2}$, $4F_{5/2}$, $4F_{3/2}$, for the 4f transition levels of Nd^{3+} and $^6H_{5/2}\rightarrow {}^4F_{7/2}$, $^6H_{5/2}\rightarrow {}^6F_{9/2}$, $^6H_{5/2}\rightarrow {}^6F_{7/2}$, $^6H_{5/2}\rightarrow {}^6F_{5/2}$, $^6H_{5/2}\rightarrow {}^6F_{3/2}$ for the 4f transition levels of Sm^{3+} respectively. From figure 5, found the absorption intensity band at 582 nm reduce as the content of Sm^{3+} increases. The combined doping does not alter the level positions of the Nd^{3+} and Sm^{3+} ions. –Moreover, the increase of Nd_2O_3 content in the glass caused absorption bands to become sharper. The optical band gap E_{opt} determined using the relation $\alpha h\nu = A\ (h\nu - E_{opt})^n$. Where: A is constant. The value of the power n shows the transition type, wherein n=2 indicates an indirect transition respectively.

Figure 7 suggests the indirect transition via plotting $(\alpha h\nu)^{1/2}$ vs. hν. Extrapolating the line (straight) to the hν axis gives the indirect band gaps of the studied samples. The values of the indirect band gaps had been (3.45, 3.4, 3.43, 3.19 and 3.41 eV). It noted that the lower optical band gap energy (E_{opt}) in a sample containing 0.75 mol % samarium oxide. The addition of rare earth oxide into the glasses increases the non-bridging oxygen and hence generates different oxidation states because of the mixed ions within the bridging oxygen.

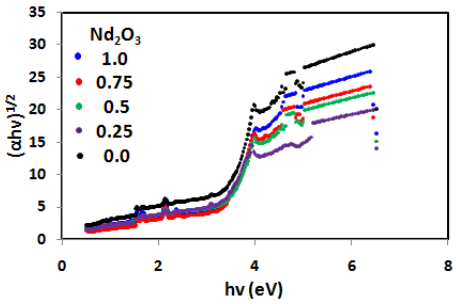

Figure 7. The indirect transition by plotting $(\alpha h\nu)^{1/2}$ vs. hν

Table 5 shows the calculated (f_{cal}), experimental (f_{exp}) oscillator strengths of the glass system containing Sm^{3+} and RMS deviation. The oscillating strengths of the various transformations (experimental and theoretical) calculated, and therefore the parameters of the Judd-Ofelt are calculated [33, 34]. The RMS deviation δ_{rms} calculated using the following relation [35-37].

$$\delta_{rms} = \sqrt[2]{\frac{\sum(f_{cal}-f_{exp})^2}{N-3}} \quad (1)$$

N is the total number of energy levels.

Table 6 shows the measured f_{exp} , theoretical f_{cal} oscillator strength of the glass system containing Nd^{3+} and RMS deviation . From table 6, the value of δ_{rms} is very low (< 1) which indicates the J-O theory is valid [38, 39]. The values of RMS imply the good fitting relating to the measured f_{exp} and the theoretical f_{cal} oscillator strengths. This sample shows a slight difference between experiment f_{exp} and calculation f_{cal}. Three Judd-Ofelt parameters of Sm^{3+} and Nd^{3+}doped glass samples obtained, Ω_2 parameter describes the environment asymmetric or Sm^{3+} and O^{2-} ligand covalence because the samarium ions found in the different coordination environment. Sometimes the samarium has the same coordination, however, there may a chance of change in the crystalline field due to the deviation in the samarium position.

Table 5. Experimental energies (Eexp), experimental (fexp) and calculated (fcal) oscillator strengths for the energy levels of the Sm^{3+} glass

$^6H_{5/2}\rightarrow$	*E*exp (cm^{-1})	Sample 2		Sample 3		Sample 4		Sample 5	
		*f*cal x10^{-6}	*f*exp x10^{-6}	*f*cal x10^{-6}	*f*exp x10^{-6}	*f*cal x10^{-6}	*f*exp x10^{-6}	*f*cal x10^{-6}	*f*exp x10^{-6}
$^6F_{3/2}$	6858	0.295	0.535	0.337	0.343	0.237	0.400	0.972	0.979
$^6F_{5/2}$	7363	0.582	0.959	0.841	0.832	0.511	0.957	1.80	1.76
$^6F_{7/2}$	8237	1.02	1.56	1.04	1.09	0.822	0.974	2.61	2.70
$^6F_{9/2}$	9380	0.681	o.869	0.591	0.537	0.532	1.01	1.63	1.51
$^6F_{11/2}$	10683	0.111	0.110	0.0914	0.0830	0.0855	0.0952	0.259	0.138
RMS x10^{-6}		0.124		0.882		0.015		0.952	

Table 6. Experimental energies (Eexp), experimental (fexp) and calculated (fcal) oscillator strengths for the energy levels of the Nd+ glass

$^4I_{9/2}\rightarrow$	*E*exp (cm–1)	Sample 1		Sample 2		Sample 3		Sample 4	
		*f*cal x10^{-6}	*f*exp x10^{-6}	*f*cal x10^{-6}	*f*exp x10^{-6}	*f*cal x10^{-6}	*f*exp x10^{-6}	*f*cal x10^{-6}	*f*exp x10^{-6}
$^4F_{3/2}$	11520.74	0.928	0.623	-------	-------	-------	-------	--------	---------
$^4F_{5/2}$	12468.83	2.49	3.21	1.59	1.64	0.871	0.911	1.07	1.08
$^4S_{3/2}$	13404.83	2.36	1.72	1.60	1.45	0.953	0.864	1.08	0.971
$^4F_{9/2}$	14705.88	0.192	0.130	0.126	0.0598	0.0732	0.0438	--------	---------
$^4G_{5/2}$	17182.13	4.21	3.06	1.92	1.39	2.30	1.67	2.54	1.82
$^4G_{7/2}$	19083.97	1.35	0.400	0.776	0.373	0.471	0.214	0.605	0.322
$^4G_{9/2}$	19607.84	0.550	0.332	0.331	0.295	0.167	0.114	0.227	0.0577
$^2G_{9/2}$	21186.44	0.390	0.105	0.237	0.112	0.117	0.115	0.159	0.292
$^2P_{1/2}$	23364.49	0.264	0.0467	0.150	0.0453	0.0606	0.0285	0.0986	0.0276
RMS x10^{-6}		1.26		0.609		0.47		0.606	

These distortions may contribute effectively to covalent or asymmetric environments. The parameters Ω_4 and Ω_6 indicate the large properties of the glass such as hardness and viscosity. In current glass systems, J-O parameter values presented in Table 7, Table 8 and follow the tendency as $\Omega_4 > \Omega_6 > \Omega_2$. The same trend observed in other glass systems [38-41]. According Jorgensen and Reisfeld [42], the Ω_λ extra affected the crystal- field asymmetry and the changes in the energy distinction relating to 4fN and 4fN—15d configuration. In other phrases, Ω_2 will increase because of the nephelauxetic impact. This occurs due to the deformation of the electronic orbital within the 4f configuration. Increase the overlap the 4f of Nd^{3+} ion and oxygen orbital induced the energy level of Nd^{3+} ion contracts and shifting inside the wavelength. Furthermore, shifting all transitions to higher wavelength indicate the presence of Nd — O linkages in the glass system. The transition $^4I_{9/2}\rightarrow {}^2G_{9/2}$ observed is greater intense than the alternative transitions which well see from the intensity of the calculated oscillator strength increases empirically and relates to the structural changes of the location of the rare-earth ions. Ω_2 rose significantly by reducing the symmetry of the rare-earth site and the more covalent its chemical bond with the ligands field. As a whole, the Ω_2 increases because of the covalence among the rare earth ion and the ligand field increases, as the symmetry lowers, and as the electric gradient relating the rare earth ion and the ligand fields increases. The higher the value of Ω_4 in the current glass indicates the higher the hardness of the glass network and the higher covalent around the sm^{3+} ions. The ratio between Ω_4 to Ω_6 indicates that all the samples containing Sm found this ratio greater than 1. These resulting analyses verify that the glass used as a laser generator.

Figure 8 shows the variation of emission intensity for the transition of Sm^{3+} -Nd^{3+} containing glasses excited at 400 nm. It clears the three peaks at 561, 599 and 647 nm, which assigned to $^4G_{5/2}\rightarrow {}^6H_{5/2}$, $^6H_{7/2}$,

$^6H_{9/2}$ transitions of Sm^{3+} ions. The intensities of the bands gradually elevated with Sm^{3+} ion attention enhanced within the samples, the glasses emit reddish-orange light. Luminescence spectra give detailed information for energy level splitting of doping ions in $Li_2O—B_2O_3—(Nd_2O_3/ Sm_2O_3)$ glasses. The luminescence spectrum of glass contains neodymium (samarium free), the luminescence vulnerable (weak) band noticed at 599 nm corresponding transitions $^4G_{7/2}\rightarrow{}^4I_{11/2}$, $^4G_{5/2}\rightarrow{}^4I_{9/2}$. Alternative Sm^{3+} ions doped glasses (free from neodymium) reveal four luminescence strong bands at 562, 599, and 646 nm. Those bands attributed $^4G_{5/2}\rightarrow{}^6H_{5/2}$, $^4G_{5/2}\rightarrow{}^6H_{7/2}$, $^4G_{5/2}\rightarrow{}^6H_{9/2}$ transitions of Sm^{3+} ions in glass network, the band intensities regular elevated Sm^{3+} ion attention increased by mixed rare earth glass network [43, 44].

Table 7. Judd-Ofelt parameters ($\Omega\lambda\times10^{-20}$ cm^2) and trends of the $\Omega\lambda$ parameters for various $Nd3^+$ glasses

Sample	$\Omega2$ x$10^{-20}cm^{-2}$	$\Omega4$ x$10^{-20}cm^{-2}$	$\Omega6$ x$10^{-20}cm^{-2}$	Trend
2	0.135	0.907	0.656	$\Omega4>\Omega6>\Omega2$
3	0.143	1.36	0.540	$\Omega4>\Omega6>\Omega2$
4	0.0312	0.772	0.485	$\Omega4>\Omega6>\Omega2$
5	0.575	2.49	1.37	$\Omega4>\Omega6>\Omega2$

Table 8. Judd-Ofelt parameters ($\Omega\lambda\times10^{-20}$ cm^2) and trends of the $\Omega\lambda$ parameters for various Sm^{3+} glasses

Sample	$\Omega2$ x$10^{-20}cm^{-2}$	$\Omega4$ x$10^{-20}cm^{-2}$	$\Omega6$ x$10^{-20}cm^{-2}$	Trend
1	0.316	1.64	1.39	$\Omega4>\Omega6>\Omega2$
2	0.0160	0.914	0.947	$\Omega6>\Omega4>\Omega2$
3	0.510	0.362	0.580	$\Omega6>\Omega2>\Omega4$
4	0.418	0.575	0.611	$\Omega6>\Omega4>\Omega2$

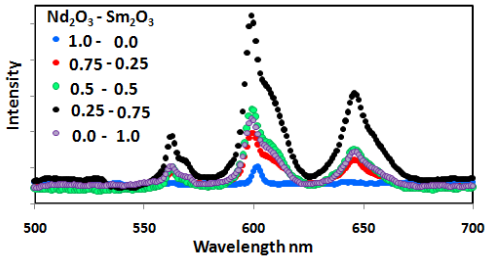

Figure 8. the emission spectra of Sm^{3+} - Nd^{3+}containing lithium borate glasses excited at 400 nm

As it appears (in Figure 9) possible Nd^{3+} ion energy $^4F_{3/2}$ level transfer to the Sm^{3+} ion $^6F_{9/2}$ level. Thereby Sm^{3+} ion excited $^6F_{9/2}$ to $^4G_{7/2}$ and subsequent de-excites to $4G_{5/2}$ via nonradiative decay and strengthens the emission transitions from Sm^{3+} ions $^4G_{5/2}$. This increases the intensity of the Sm^{3+} emission lines expenses the Nd^{3+} emission lines. The branching ratio B value found highest the transition $^4G_{5/2}\rightarrow{}^6H_{7/2}$ (near orange emission) in the glasses and found that the value B for the transition $^4G_{5/2}\rightarrow{}^6H_{7/2}$ is 60, 57 and 51 % respectively. In many other glass systems, the highest B value of this transition reported from Sm^{3+} ions. Finally the general analysis of the current results suggests that the combined interaction of the Sm^{3+} ions containing Nd^{3+} ions significantly improves the transfer of orange emissions from Sm^{3+} ions into the studied glass system and makes the glasses suitable for orange emissions devices. Besides, the replacing 0.25 mole% Sm^{3+} by Nd^{3+} gives the highest intensity of the emitted radiation.

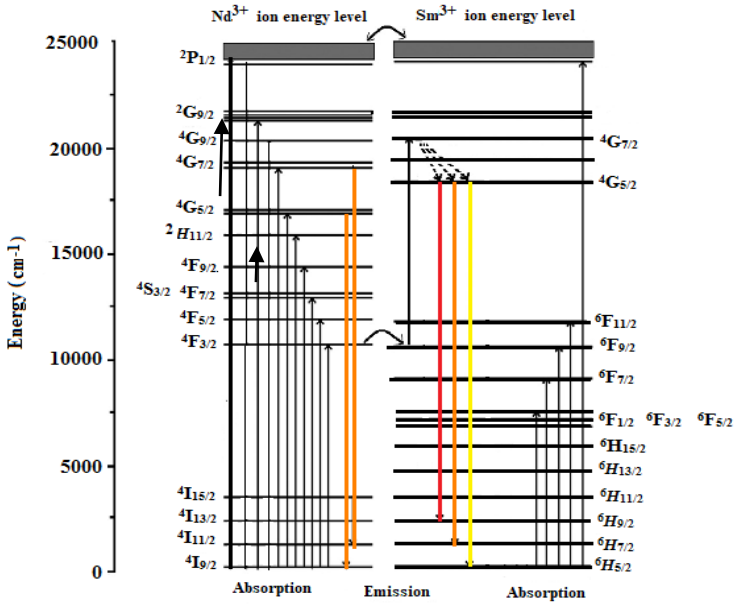

Figure 9. The energy level transition of Nd^{3+}, Sm^{3+} ions

4. CONCLUSION

Samarium and neodymium ions doped Lithium borate glass prepared and studied. The density of glass samples indicates that the density measurement increases as samarium content increase and the distinction among the experimental and calculated density increase as the samarium content increase. The functional vibration groups within the glass matrix have studied and indicate the addition of rare earth ion transfer the BO_3 vibration groups to BO_4 and forming nonbridging oxygen. Judd—Ofelt (J—O) principle has applied and evaluates J—O intensity parameters. The general analysis of the results of the present study optical properties (absorption and emission) indicates that these glass samples are answerable for orange. Based on the results obtained from the J-O analysis, the parameters concluded that the glass under study is a promising luminescent and laser material. The current glasses in the study have the potential to act like an orange emission device as well as photovoltaic applications.

REFERENCES

[1] Sun X.-Y., *et al*, "Luminescent properties of Tb3+-activated B2O3–GeO2–Gd2O3 scintillating glasses," *J. Non-Cryst. Solids*, vol. 379, pp. 127-130, 2013.
[2] Thomas S., *et al*, "Spectroscopic and dielectric studies of Sm3+ ions in lithium zinc borate glasses," *J. Non-Cryst. Solids*, vol. 376, pp. 106-116, 2013.
[3] Babu, A. M., Jamalaiah, B.C., Sasikala, T., Saleem, S.A., Moorthy, L. R., "Absorption and emission spectral studies of Sm3+ doped lead tungstate glasses," *J. Alloys Compd*, vol. 509, no. 14, pp. 4743-4747, 2011.
[4] Jamalaiah B.C., Kumar J. S., Babu A. M., Suhasini T., Moorthy L. R., "Photoluminescence properties of Sm3+ in LBTAF glasses," *J. Lumin*, vol. 129, no. 4, pp. 363-369, 2009.
[5] Lakshminarayana G., Qiu J., "Photoluminescence of Pr3+, Sm3+ and Dy3+-doped SiO2–Al2O3–BaF2–GdF3 glasses," *J Alloys Compd*., vol. 476, no. 1-2, pp. 470-476, 2009.
[6] Som T., Karmakar B., "Infrared-to-red upconversion luminescence in samarium-doped antimony glasses," *J. Lumin*, vol. 128, no. 12, pp. 1989-1996, 2008.
[7] Kindrat I.I., Padlyak B.V., Drzewiecki A., "Luminescence properties of the Sm-doped borate glasses," *J. Lumin*, vol. 166, pp. 264–275, 2015.
[8] Tripathi G., Rai V.K., Rai S.B., "Optical properties of Sm3+:CaO-Li2O-B2O3-BaO glass and codoped Sm3+:Eu3+," *Appl. Phys. B*, vol. 84, no. 3, pp. 459-464, 2006.
[9] Biju, P.R., Ajithkumar, G., Jose, G., Unnikrishnan, N.V., "Spectroscopic studies of Sm3+ doped phosphate glasses Bull," *Bulletin of Materials Science*, vol. 21, no. 5, pp. 415-419, 1998.
[10] Lakshminarayana G., Buddhudu S., "Spectral analysis of Sm3+ and Dy3+: B2O3–ZnO–PbO glasses," *Physica B*, vol. 373, no. 1, pp. 100-106, 2006.
[11] Sudhakar K.S.V., *et al*, "Influence of modifier oxide on spectroscopic and thermoluminescence characteristics of Sm3+ ion in antimony borate glass system," *J. Lumin*, vol. 128, no. 11, pp. 1791-1798, 2008.

[12] Becker, P., "Thermal and optical properties of glasses of the system Bi2O3 – B2O3," *Crystal Research and Technology: Journal of Experimental and Industrial Crystallography*, vol. 38, no. 1, pp.74-82, 2003.
[13] Bajaj, A., *et al*, "Structural investigation of bismuth borate glasses and crystalline phases," *J. Non-Cryst. Solids*, vol. 355, no. 1, pp. 45-53, 2009.
[14] Zhu X., Mai C., Li M., "Effects of B2O3 content variation on the Bi ions in Bi2O3–B2O3–SiO2 glass structure," *J. Non-Cryst. Solids*, vol. 388, pp. 55-61, 2014.
[15] Chewpraditkul,W., Shen,Y., Chen,D., Yu, B., Prusa, P., Nikl,M., Beitlerova,A., Wanarak,C., "Luminescence and scintillation of Ce3+-doped high silica glass," *Opt. Mater.*, vol. 34, no. 11, pp. 1762-1766, 2012.
[16] Wantana N., *et al*, "Energy transfer from Gd3+ to Sm3+ and luminescence characteristics of CaO–Gd2O3–SiO2–B2O3 scintillating glasses, *J. Lumin*., vol. 181, pp. 382–386 , 2017.
[17] Ramteke D.D., Ganvir V. Y., Munishwar S. R., Gedam R. S., "Concentration effect of Sm3+ Ions on structural and luminescence properties of lithium borate glasses," *Physics Procedia*, vol. 76, pp. 25–30, 2015.
[18] Huang L., Jha A., Shen S., "Spectroscopic properties of Sm3+-doped oxide and fluoride glasses for efficient visible lasers (560–660 nm)," *Opt. Commun*., vol. 281, no. 17, pp. 4370-4373, 2008.
[19] Gorller-Walrand, C., Binnemans, K., in: Gschneidner, K.A., Eyring, L. (Eds.), *Handbook on the Physics and Chemistry of Rare Earths*, pp. 101–264. chapter 167, North-Holland Publishers, Amsterdam, 1998,.
[20] Mahato K.K., Rai D.K., Rai S.B., "Optical studies of Sm3+ doped oxyfluoroborate glass," *Solid State Commun*., vol. 108, no. 9, pp. 671-676, 1998.
[21] Lin H., *et al*, "Spectral parameters and visible fluorescence of Sm3+ in alkali–barium–bismuth–tellurite glass with high refractive indexm," *J. Lumin.*, vol. 116, no. 1-2, pp. 139-144, 2006.
[22] Praveena R., Venkatramu V., Babu P., Jayasankar C.K., "Fluorescence spectroscopy of Sm3+ ions in P2O5–PbO–Nb2O5 glasses," *Physica B: Condensed Matter*, vol. 403, no. 19-20, pp. 3527-3534, 2008.
[23] Gatterer, K, *et al*, "Suitability of Nd(III) absorption spectroscopy of probe the structure of glasses from the ternary system Na2O-B2O3-SiO2," *J. Non-Cryst. Solids*, vol. 231, no. 1-2, pp. 189-199, 1998.
[24] Maumita Das, Annapurna K, Kundu P, Dwivedi RN, Buddhudu S., "Optical spectra of Nd3+:CaO–La2O3–B2O3 glasses," *Materials Letters*, vol. 60, no. 2, pp. 222-229, 2006.
[25] .Rao, T.G.V.M., *et al*, "Optical and structural investigation of Sm3+–Nd3+ co-doped in magnesium lead borosilicate glasses," *Journal of Physics and Chemistry of Solids*, vol. 74, no. 3, pp. 410–417, 2013.
[26] Joshi, J. C., SHI, J. A., Belwalab, R., Joshi, C., Pandey, N. C., "Non-radiative energy transfer from Sm3+→Nd3+ in sodium borate glass," *j. Phys Chem. Solids*, vol. 39, no. 5, pp. 581-584, 1978.
[27] Wang F., *et al*, "The influence of TeO2 on thermal stability and 1.53μm spectroscopic properties in Er3+ doped oxyfluorite glasses," *Spectrochim Acta A: Mol. Biomol. Spect*., vol. 150, pp. 162–169, 2015.
[28] Dahshan, A., "Thermal stability and crystallization kinetics of new As-Ge-Se-Sb glasses," *J. Non-Cryst. Solids*, vol. 354, no. 26, pp. 3034-3039, 2008.
[29] Tandon R.P., Hotchandani S., "Electrical conductivity of semiconducting tungsten oxide glasses," *Phys. Status Solidi A*, vol. 185, no. 2, pp. 453-460, 2001.
[30] Qiu H.-H., Mori H., Sakata H., Hirayma T., "Electrical conduction of glasses in the system Fe2O3-Sb2O3-TeO2," *J. Ceram. Soc. Jpn*., vol. 103, no. 1193, pp. 32-38, 1995.
[31] Khalifa F.A., El Batal H.A., Azooz A., "Infrared absorption spectra of gamma irradiated glasses of the system Li2O-B2O3-Al2O3," *Indian J. Pure Ap. Phy*., vol. 36, no. 6, pp. 314-318, 1998.
[32] Rai A. and Rai V. K., "Optical properties and upconversion in Pr3+ doped in aluminum, barium, calcium fluoride glass—I," *Spectrochimica Acta Part A: Molecular and Biomolecular Spectroscopy*, vol. 63, no. 1, pp. 27-31, 2006.
[33] Judd B.R., "Optical absorption intensities of rare-earth ions," *Phys. Rev*., vol. 127, no. 3, pp. 750-761, 1962.
[34] Ofelt G.S., "Intensities of crystal spectra of rareearth ions," *J. Chem. Phys*.. vol. 37, no. 3, pp. 511-520, 1962.
[35] Padlyak B.V., Kindrat I.I., Protsiuk V.O., Drzewiecki A., "Optical spectroscopy of Li2B4O7, CaB4O7 and LiCaBO3 borate glasses doped with europium," *Ukr. J. Phys. Opt*., vol. 15, no.3, pp. 103-117, 2014.
[36] Joseph X., George R., Thomas S., Gopinath M., Sajna M.S., Unnikrishnan N.V., "Spectroscopic investigations on Eu3+ ions in Li–K–Zn fluorotellurite glasses," *Opt. Mate*., vol. 37, pp. 552-560, 2014.
[37] Mohamed E. A., Ratep A., Abdel-Khalek E. K., Kashif I., "Crystallization kinetics and optical properties of titanium–lithium tetraborate glass containing europium oxide," *Appl. Phys. A*, vol. 123, no. 3, pp. 479-, 2017.
[38] Kumar K. A., Babu S., Prasad R., Damodaraiah S., Ratnakaram Y.C., "Optical response and luminescence characteristics of Sm3+ and Tb3+/sm3+ co-doped potassium-fluoro-phosphate glasses for reddish-orange lighting applications," *Materials Research Bulletin*, vol. 90, pp. 31-40, 2017.
[39] Babu, S., *et al*, "Investigations on luminescence performance of Sm3+ ions activated in multi-component fluorophosphates glasses," *Spectrochim. Acta Part A*, vol. 122, pp. 639–648 , 2014.
[40] Sobczyk M., Szymański D., Guzik M., Legendziewicz J., "Optical behaviour of samarium doped potassium yttrium double phosphates," *J. Lumin*., vol. 169, pp. 794–798, 2016.
[41] Thomas S., *et al*., "Optical properties of Sm3+ ions in zinc potassium fluorophosphate glasses," *Opt. Maters*, vol. 36, no. 2, pp. 242–250, 2013.
[42] Jorgensen C K, Reisfeld R., "Judd-Ofelt parameters and chemical bonding," *J. Less-Common Metals*, vol. 93, no. 1, pp. 107-112, 1983.
[43] Herrmann, A., Ehrt, D., "Time-resolved fluorescence measurements on Dy3+ and Sm3+doped glasses," J. *Non-Cryst. Solids*, vol. 354, no. 10-11, pp. 916–926, 2008.
[44] Malchukova E., Boizot B., Ghaleb D., "Optical properties and valence state of Sm ions in aluminoborosilicate glass under β-irradiation," *J. Non-Cryst. Solids*, vol. 353, no. 24-25, pp. 2397–2402, 2007.